ECHAHID HAMMA LAKHDAR UNIVERSITY - EL-OUED
Under the Supervision of the DGRSDT and in collaboration with the CRTI
International Pluridisciplinary PhD Meeting (IPPM'20)
23-26, 2020 1st Edition, February
Theme: Modern Technology and Fineness Life

4 to 5 pages

Biosynthesis and characterization of Iron oxide nanoparticles by Mentha Pulegium .L leaf extract

Abderrhmane Bouafia [a,b,*], Salah Eddine Laouini [a,b]

[a] Department of Process engineering, Faculty of Technology, University of Echahid Hamma Lakhdar, El Oued 39000, Algeria
[b] Lab. VTRS, Faculty of Technology, Univ. El-Oued, El oued 39000, Algeria
E-mail: abdelrahmanebouafia@gmail.com, salah_laouini@yahoo.fr

Abstract

In this study, green synthesis of iron oxide nanoparticles was successfully prepared from Mentha Pulegium L leaves extract. The effect of different ferric chloride concentrations on the nanoparticles' iron oxide formation was studied. The obtained nanoparticles were characterized by UV-Vis, FT-IR, XRD, SEM and EDAX techniques are used for this purpose. UV-Vis spectra showed maximum absorption at range 275-301 nm related to the iron oxide. FTIR spectra exhibit a two weak peak at 510 and 594 cm^{-1} attributed to iron oxide NPs vibration, confirming the formation nanoparticles XRD confirmed the crystalline nature of Fe_3O_4 and α-Fe_2O_3 NPs with average size ranged in 22-34 nm.SEM showed that the green synthesizing Iron oxide nanoparticles having in general as cubical shape. As a result, the use of Mentha Pulegium L leaves extract offers its ease, fast, low cost and friendly to the environment compared to other methods.

Keywords: Iron Oxide; Mentha Pulegium L; Ferric Chloride; Green Synthesis; XRD.

1. Introduction

As a result of the terrible environmental pollution that has hit the world, green technology and chemistry have become more common and used.

Green synthesis is an advance over physical and chemical methods because it is environmentally friendly and easy to implement for large-scale synthesis. This method does not require the use of high pressure, temperature, energy and a toxic chemical [1].

In recent years, the interest in ferrous nanomaterials (IONPs) has increased due to its very diverse properties, high catalytic activities and high intrinsic interactivity of its surface sites with great interest from researchers in various fields.

Iron oxides are available in nature and can be easily synthesized in the laboratory. There are about 16 forms of iron oxides, including hydroxides, oxides, and hydroxides. Oxidation and reduction behavior Linked to PH and implements the water interactions between the minerals. The crystal clamps and valence are different only, otherwise, the general constitution of Fe, O, and/or OH is similar.

2. Materials and Methods

2.1. Preparation of the leaf extract

Leaves of Mentha Pulegium L were collected from local fields in the region of El Oued (Southeast of Algeria). Fresh leaves were washed and dried in a shade at room temperature for 5-7 days, and then crushed to obtain a fine powder, The plant material was extracted by the maceration method. The extract was prepared by putting 10g of powder's leaves with 100ml of distilled water in a 250 ml glass beaker. The mixture was stirred steadily for 24 hours at room temperature. The extract was filtered using a filter paper (Whatman No: 42) and stored in a glass container airtight at 4 °C for further use.

2.2. Synthesis of iron oxide nanoparticles by Mentha Pulegium extract

Iron oxide nanoparticles were synthesized by a modified protocol from previous researches [2-7]. Briefly, by adding with four different concentrations (0.01,0.04,0.07, and 0.1M) of the ferric chloride solution ($FeCl_3$) to the leaf extract in a 1:10 volume ratio between the leaf extract and ferric chloride was taken as 20 ml/200 ml in a 250 mL flask. IONPs were immediately obtained with the reduction process. The mixture was continuous stirring at 75°C for 1 hour. The formation of iron oxide NPs is indicated by a change in the color of the mixture solution of light brown to the dark black. the reasonable mechanism of iron oxide nanoparticles formation may be due to the reduction of iron ions that takes place together with the phenolic compounds in the Mentha Pulegium L leaf extract.

2.3. Characterization of Iron oxide nanoparticles

The obtained malachite samples were confirmed by powder X-ray diffraction in the 2θ angles ranging from 20° to 90°. The morphologies of as-synthesized IONPs samples were characterized by using a scanning electron microscope (SEM, S-3400N). FT-IR spectra were recorded on a fourier transmission infrared spectrometry (FT-IR, ATR device) at wavenumbers 400–4000 cm^{-1}. The UV–vis transmission spectra were determined with a spectrophotometer (Shimadzu-1800).

3. Results and discussion

The UV-Vis spectra of iron oxide nanoparticles synthesized using a Mentha Pulegium L leaf extract are shown in Fig.1. As can be seen from this figure, one peaks of maximum absorption are exhibited .The absorption peak at 275-301 nm gives a clue that iron oxide nanoparticles may be formed [8, 9].

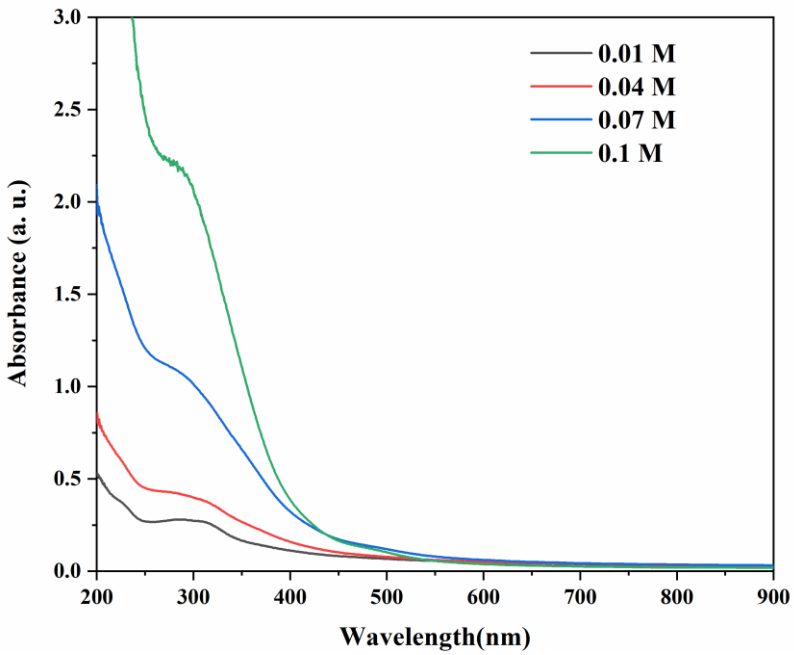

Fig.1.UV–Vis absorption spectrum of Iron oxide nanoparticles synthesized

The estimated optical band gap (Eg) of iron oxide nanoparticles can be determined by extrapolation from the absorption edge which is given using Tauc's relation Eq.(1) [10, 11]:

$$(\alpha h\nu)^2 = A\left(h\nu - E_g\right) \qquad (1)$$

where α is the absorption coefficient, A is constant, hν is the energy of light and n is a constant depending on the nature of the electron transition [12]. iron oxide NPs has a direct band gap (n = 2). the plot of $(\alpha h\nu)^2$ versus hν. The optical band gap of samples is shown in Table 1.

Fig. 2(a) gathers the FT-IR spectrum of Mentha Pulegium L leaf extract with different spectra of nanoparticles prepared with different ration. (Fig. 2(a) a) shows the FT-IR spectrum of Mentha Pulegium L leaf extract, this spectrum depicted some peaks at 3455,2971,2947, 1744, 1364, 1218 and 1088 cm^{-1}. The broadband, at 3455 cm^{-1}, is due to the O–H group stretching vibration .Significant peaks were found at (2971, 2947) cm^{-1} ascribed to methyl group, The absorption peaks situated around 1744 and 1364 cm^{-1} correspond to the stretching vibrations of C=C, C–C, and C–O of the aromatics cycles . Weak bands at 1218 and 1088 cm^{-1} indicate the presence of C–H and C–O stretching of alcohols, carboxylic acids, ester and, ether groups respectively.By comparing the spectrum of the as iron oxide nanoparticles each other, Fig. 2(b) shows a peek at 510 and 594 cm^{-1}, which, corresponding to the Fe-O stretching band of iron oxide (Fe_2O_3 et Fe_3O_4 NPs) [13-15].

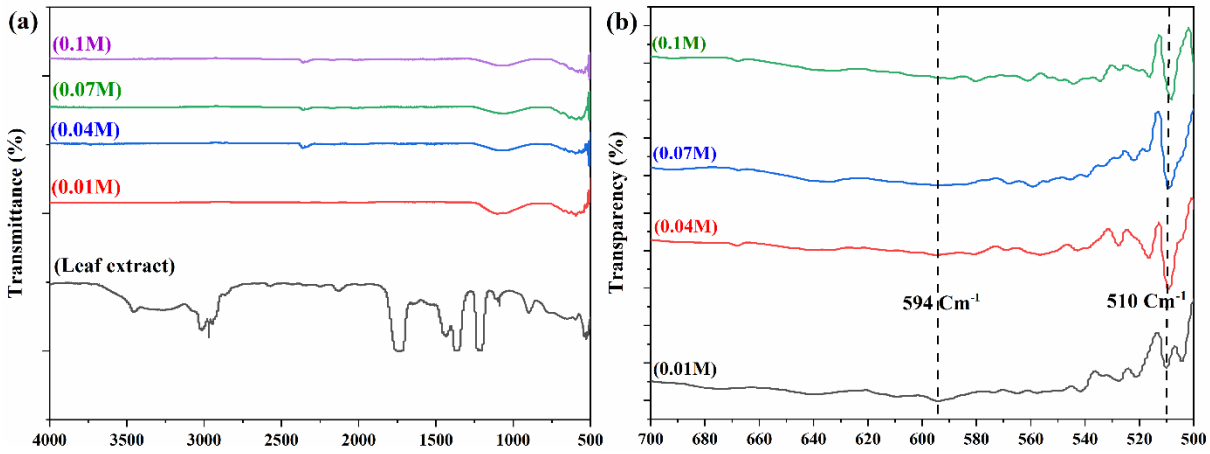

Fig.2. (a) FT-IR spectra of Mentha Pulegium L leaf extract and as synthesized iron oxide nanoparticles powder with different ferric chloride concentration and (b) FT-IR spectra Illustrative at range 500 to 700 Cm^{-1},focuses on Fe-O bonds, of synthesized iron oxide nanoparticles

The Fig.3 exhibits typical XRD patterns of synthesized and annealed at 500°C iron oxide nanoparticles with different concentrations of ferric chloride. Show in Fig.3 the spectrum indicates the presence of Hematite α-Fe_2O_3 and Magnetite Fe_3O_4 mixture. As depicted by the peaks at 2θ values of 24.13°, 33.15°, 35.45 °, 40.70°, 49.47°, 54.04°,57.50°, 62.90° and 63.98° which correspond to the crystal planes of (012), (104), (110), (113), (024), (116), (122), (214), and (300) of Hematite a-Fe_2O_3 phase [14]. All the reflection peaks are matching well with the expected to the rhombohedral structure of α-Fe_2O_3, respectively. Those planes accord well with the (JCPDS Card No. 00-024-0072). Whereas the peaks at 2θ value of 30.25°,35.45 °,43.20°, 53.60°, 57.26°, and 62.90° correspond to the planes of (011), (112), (202), (004), (321), and (224) of Orthorhombic crystal structures of magnetite Fe_3O_4 much well with the (JCPDS Card No. 01-075-1609) [15]. In our study, two iron oxide phases were obtained, namely magnetite and hematite, which are the best in the iron oxide family, according to previous studies.

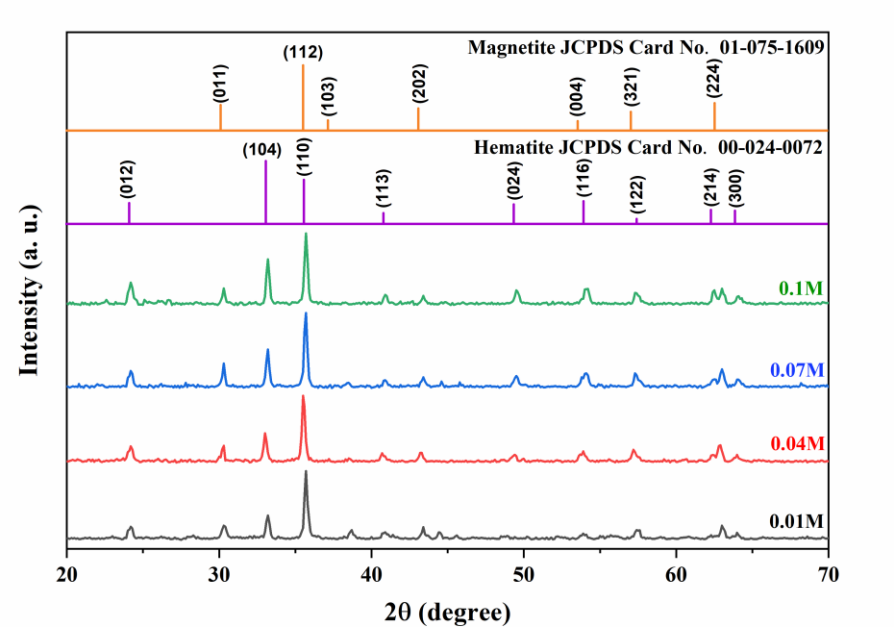

Fig.3.XRD patterns of iron oxide nanoparticles synthesized

In Table 1 it was reported the variation of the crystallite size of the two NPs (α-Fe_2O_3 and Fe_3O_4) .

Table 1 . Size and optical band gap of iron oxide nanoparticles synthesized at different ferric chloride concentration

Samples	Magnetite Fe_3O_4 NPs size (nm)	Hematite α-Fe_2O_3 NPs size (nm)	Optical band gap Eg (eV)
0.01 M	24.67 ± 1.07	24.45 ± 1.71	2.96
0.04 M	27.63 ± 1.45	25.38 ± 1.22	2.27
0.07 M	34.28 ± 2.36	28.83 ± 3.17	2.48
0.1M	33.46 ± 3.15	27.82 ± 2.45	2.92

The formation of iron oxide NPs and their morphological dimensions were studied using the SEM. Fig. 4 (a-d) exhibits SEM images of the synthesized iron oxide (IONPs). It is observed that most of them are cubic in nature and irregular shaped. Note it's free of agglomeration For the mixture of α-Fe_2O_3 and Fe_3O_4 nanoparticles (Fig. 4 c and d); further, the particles are agglomerated to form foam like a bunch of particles. This also shows the formation of a cubic shape of ferrous nanoparticles as shown in Fig.4 (a and b).

Further analysis of iron oxide nanoparticles, by EDAX, as shown in (Fig.4 e) its associated data, confirms the presence of iron and oxygen, with the weight percentage of about 45.57% Fe and 54.40% O.

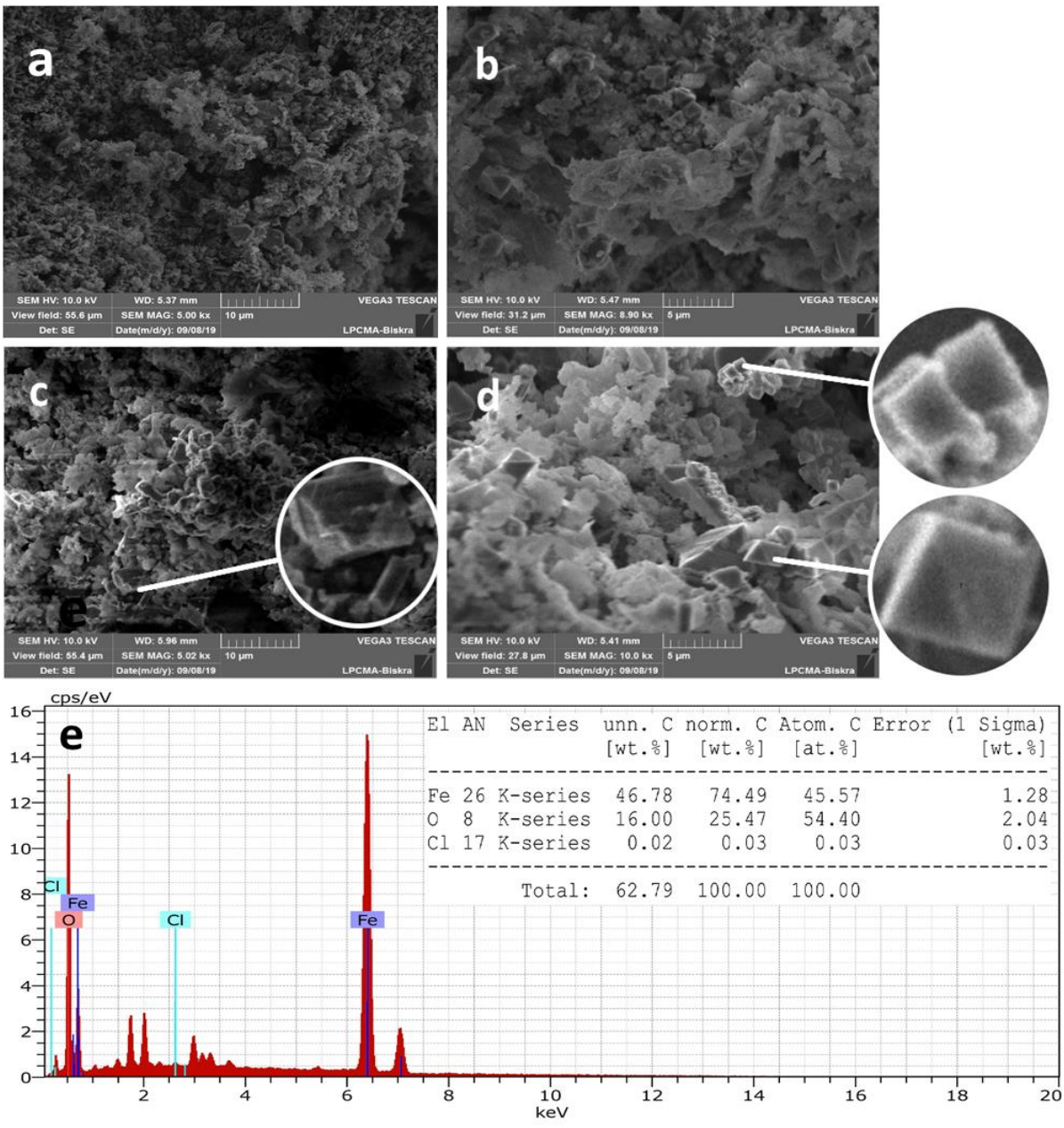

Fig.4.SEM images of green synthesized IONPS nanoparticles: a) 0.01 M, b) 0.04 M,c)0.07M , d) 0.1M and e) EDAX of iron oxide nanoparticles.

4. Conclusion

Iron oxide has been successfully prepared by a simple approach. The prepared iron oxide product has a cubical structure and narrow band gap, which could effectively absorb visible light and might have potential applications in a photocatalyst. Results showed the variation of the molar amount of Fe precursor allows us to strictly control the size and shape of the iron oxide, which is suitable for large scale production.

References

[1] R.B. Malabadi, S.L. Naik, N.T. Meti, G.S. Mulgund, K. Nataraja, S.V. Kumar, Research in Biotechnology 3(5) (2012).
[2] M.S. Kubde, S. Khadabadi, I. Farooqui, S. Deore, Rep Opin 2(3) (2010) 91-8.
[3] M. Pattanayak, P. Nayak, World J. Nano Sci. Technol 2(1) (2013) 06-09.
[4] A. Singh, D. Jain, M. Upadhyay, N. Khandelwal, H. Verma, Dig J Nanomater Bios 5(2) (2010) 483-489.
[5] M. Ramya, M.S. Subapriya, Int J Pharm Med Biol Sci 1(1) (2012) 54-61.
[6] S. Li, Y. Shen, A. Xie, X. Yu, L. Qiu, L. Zhang, Q. Zhang, Green Chemistry 9(8) (2007) 852-858.
[7] T. Shahwan, S.A. Sirriah, M. Nairat, E. Boyacı, A.E. Eroğlu, T.B. Scott, K.R. Hallam, Chemical Engineering Journal 172(1) (2011) 258-266.
[8] P. Karpagavinayagam, C. Vedhi, Vacuum 160 (2019) 286-292.
[9] S. Groiss, R. Selvaraj, T. Varadavenkatesan, V. Ramesh, 2016.
[10] A. Lassoued, M.S. Lassoued, B. Dkhil, S. Ammar, A. Gadri, Physica E: Low-dimensional Systems and Nanostructures 97 (2018) 328-334.
[11] W.B. Soltan, S. Nasri, M.S. Lassoued, S. Ammar, Journal of Materials Science: Materials in Electronics 28(9) (2017) 6649-6656.
[12] R. Beranek, H. Kisch, Photochemical & Photobiological Sciences 7(1) (2008) 40-48.
[13] M. Masikini, University of the Western Cape, 2010.
[14] D. Yufanyi, A. Ondoh, J. Foba-Tendo, K. Mbadcam, Am. J. Chem 5(1) (2015) 1-9.
[15] S. Karlapudi, C. Prasad, S. Himagirish Kumar, N. Jyothi, P. Venkateswarlu.